HITACHI

GE Hitachi Nuclear Energy

Richard E. Kingston
Vice President, ESBWR Licensing

P.O. Box 780 M/C A-65
Wilmington, NC 28402-0780
USA

T 910.675.6192
F 910.362.6192
rick.kingston@ge.com

MFN 09-778, Revision 2 Docket No. 52-010

March 11, 2010

U.S. Nuclear Regulatory Commission
Document Control Desk
Washington, D.C. 20555-0001

Subject: **Revised Response (Revision 2) to Portion of NRC Request for Additional Information Letter No. 391 Related to Design Control Document (DCD) Revision 6 – Fuel Racks - RAI Number 9.1-144**

The purpose of this letter is to submit the GE Hitachi Nuclear Energy (GEH) revised response (Revision 2) to the U.S. Nuclear Regulatory Commission (NRC) Request for Additional Information (RAI) 9.1-144 sent by NRC Letter 391, Reference 1.

The GEH revised response (Revision 2) to RAI 9.1-144 is provided in Enclosure 1. Enclosure 2 contains the LTR markups associated with this revised response. The purpose of this revision is solely to remove proprietary information markings from Enclosures 1 and 2. Since the submittal of the first revision of this response, as provided by Reference 2, GEH has determined that the response and associated markups contain no proprietary information.

If you have any questions or require additional information, please contact me.

Sincerely,

FOR

Richard E. Kingston
Vice President, ESBWR Licensing

References:

1. MFN 09-725, Letter from U.S. Nuclear Regulatory Commission to Jerald G. Head, *Request for Additional Information Letter No. 391 Related to Design Control Document (DCD) Revision 6*, November 9, 2009
2. MFN 09-778 Revision 1, Revised Response (Revision 1) to Portion of NRC Request for Additional Information Letter No. 391 Related to Design Control Document (DCD) Revision 6 - Fuel Racks - RAI Number 9.1-144, January 26, 2010

Enclosures:

1. Revised Response (Revision 2) to Portion of NRC Request for Additional Information Letter No. 391 Related to Design Control Document (DCD) Revision 6 – Fuel Racks - RAI Number 9.1-144
2. Revised Response (Revision 2) to Portion of NRC Request for Additional Information Letter No. 391 Related to Design Control Document (DCD) Revision 6 – Fuel Racks - RAI Number 9.1-144 – LTR Markups

cc:

AE Cubbage	USNRC (with enclosures)
JG Head	GEH/Wilmington (with enclosures)
DH Hinds	GEH/Wilmington (with enclosures)
TL Enfinger	GEH/Wilmington (with enclosures)
eDRF Section	0000-0110-4462 (response)
	0000-0114-9034 (markups)

Enclosure 1

MFN 09-778, Revision 2

Revised Response (Revision 2) to Portion of NRC Request for Additional Information Letter No. 391 Related to Design Control Document (DCD) Revision 6

Fuel Racks

RAI Number 9.1-144

NRC RAI 9.1-144

LTR NEDE-33373P, rev. 3 states that the load combinations shall be per Appendix D to SRP 3.8.4 and the stress limits shall be in accordance with ASME B&PV Code, Section III, Division I, Subsection NF and Appendix F corresponding to the design by analysis for Class 3 plate and shell type supports. However, in the Service Level D analysis, the applicant made an assumption that the maximum accident temperature T_a of 250F will not be concurrent with the SSE load; therefore, T_a was not included in the Level D load combination. Based on this assumption in the Level D analysis, the applicant concluded that the racks will not impact the pool wall liners during an SSE event.

Since the cooling system for the spent fuel pool is not a safety-related system, it can not be relied upon to provide the required cooling during an SSE event. Therefore, the applicant's assumption for not including T_a in the Level D load combination appears un-justifiable. Furthermore, the staff estimated that if T_a were included in the Level D load combination, during an SSE event, the racks would impact the pool wall liners, which violates the design requirement for the analysis that no interaction is allowed between the racks and pool walls.

Based on the above discussion, the staff requests that:

1) *the applicant provide justifications for not including the T_a in ASME Service Level D load combination, and demonstrate the racks will not impact the pool wall liners during an SSE event concurrent with T_a;*

2) *the applicant demonstrate the effect of thermal gradient based on the Service Level D load combination will not impact the functionality of the racks by following the guidance provided in Section 1.4 (the 3rd sentence of the 1st paragraph) of Appendix D to SRP 3.8.4.*

3) *Provide clarification of terms used in Section 1.6.5.1 such as R-16, BP-26, etc., which can be best illustrated by providing a schematic plan view of the layout of racks in the pool including the gaps with the pool walls.*

GEH Response (Revision 2)

1) The effects of the maximum pool temperature have been conservatively included in the Level D load combinations presented in Table 1-5 of LTR NEDC-33373P. The table has been updated to reflect inclusion as seen in the attached markup.

   The effect of maximum thermal expansion in combination with the seismic displacement is now shown in LTR NEDC-33373P in Section 1 for the spent fuel storage racks. The calculated results are:

Total Displacement N-S = 39.5 mm +2.5(4.43 mm) - 2(3 mm) = 44.6 mm < 92 mm

Total Displacement East wall = 39.5 mm +2(3.56 mm) - 1.5(3 mm) = 51.5 mm < 60 mm

In the N-S direction, the minimum clearance to the fuel pool wall has increased from 42 mm to 92 mm. This increase can be accommodated since the tolerance in the N-S pool dimension has been decreased by 100 mm (the minus tolerance was changed from 300 mm to 200 mm per Table 2.16.7-1 in Tier 1 of DCD Revision 6), thus increasing the fuel pool dimension in the N-S direction by 100 mm. Since the pool dimensions started with a relatively large tolerance, tightening the tolerance will not be an issue in view of the accurate alignment equipment that is commercially available.

At the east wall, the racks will be placed with a minimum gap of 60 mm to accommodate seismic and thermal expansion.

Since the calculated total displacements are less than the minimum clearances between the fuel storage racks and pool walls, no contact will occur.

Sections 2 and 3 of the LTR were reviewed for applicability of inclusion of T_a in the Level D load combination for the buffer pool rack designs. It was determined that the effects of pool temperature needed to be included. Therefore, the appropriate sections of the LTR have been updated to reflect inclusion as seen in the attached markups. Section 4 of the LTR is not impacted.

2) The referenced sentence says, “The temperature gradient across the rack structure that results from the differential heating effect between a full and an empty cell should be indicated and incorporated in the design of the rack structure.”

As demonstrated in the Thermal-Hydraulic analysis for the fuel storage racks (Section 5 of LTR NEDC-33373P), heat from fuel is removed by water stratification through the racks. With water acting as the medium for heat removal, there are no significant temperature gradients between a storage location occupied by spent fuel and an empty cell.

This is demonstrated by conservatively considering the worst case temperature differential. In the abnormal case, the maximum water temperature (and conservatively, the maximum rack wall temperature) at rack exit is 73.03°C (section 5.3.2 of LTR NEDC-33373P). Compared to the water inlet temperature of 46.3°C (section 5.2.2.2 of LTR NEDC-33373P), a maximum differential of 26.73°C is calculated. This is the maximum temperature gradient possible between a full cell and an adjacent empty cell.

GEH has performed simplified calculations to estimate the impact of this temperature gradient on the fuel racks. The calculation conservatively assumes that the temperature gradient occurs between two adjacent cells such that the total differential thermal expansion occurs across the width of a single cell. It further conservatively assumes that the uppermost section of the affected fuel cell is free to rotate as a result of the differential thermal expansion and is not restrained by the

rest of the fuel rack structure. The calculation evaluates the uppermost section of a fuel cell on the perimeter of the rack since this location has the smallest nominal gap between the fuel cell walls and the fuel bundles. The result of the calculation is that the decrease in the gap between the fuel bundle and the fuel cell walls is less than 44% of the nominal gap (approximately 8 mm gap reduction versus approximately 18.3 mm nominal gap size). Therefore, the distortion of the fuel racks associated with this thermal gradient would not cause the rack walls to contact the stored fuel bundles and has no effect on the integrity of the fuel bundle.
It should be pointed out that the material between the active fuel ("hot") region of adjacent cells is borated stainless steel. This material is not credited for providing structural integrity to the fuel storage racks.

3) LTR NEDC-33373P Figure 1-1 is added to provide clarification of terms used and illustrate by providing a schematic plan view of the rack and base plates in the pool including the gaps with the pool walls as shown in the attached markup.

The LTR markup pages are replaced in their entirety by this revised response.

DCD/LTR Impact (Revision 2)

No DCD changes will be made in response to this RAI.

LTR NEDO-33373 (formerly NEDC-33373P) will be revised as described and as shown in the attached markups. The following sections and tables will be revised: 1.1.1, 1.4.5.3, 1.4.6, Table 1-5, Table 2-5, 2.4.7, 2.5.1, Table 3-5, 3.4.7, 3.5.1, 5.2.3. In addition, a new Figure 1-1 has been added to the LTR.

Enclosure 2

MFN 09-778, Revision 2

Revised Response (Revision 2) to Portion of NRC Request for Additional Information Letter No. 391 Related to Design Control Document (DCD) Revision 6

Fuel Racks

RAI Number 9.1-144

LTR Markups

1. DYNAMIC LOAD ANALYSIS FOR SPENT FUEL RACKS IN THE SPENT FUEL POOL

1.1 INTRODUCTION

1.1.1 Purpose

The purpose of this document is to analyze the dynamic behavior and to present the structural analysis of Spent Fuel High Density Fuel Storage Racks (FSR) for the Spent Fuel Pool located in the Fuel Building (FB) of the ESBWR.

The layout of the FSR and the associated base plates is shown in Figure 1-1. The FSR are structures fabricated from stainless steel and borated stainless steel plates forming cells to house the spent fuel assemblies. The FSR are freestanding racks on the floor of the Spent Fuel Pool at EL -10000. The analysis evaluates the ten-year fuel storage configuration. Twenty (20) FSR will be located in the Spent Fuel Pool, providing a total of 3504 storage spaces. Two sizes of FSR are analyzed: 15x12 cell and 14x12 cell.

The configuration being analyzed consists of the 20 FSR joined to each adjacent FSR with link devices which couple the horizontal displacements. Two levels of links are analyzed between racks. At the lower level, the feet of adjacent FSR are coupled in the both horizontal directions with a bearing pad resting on the pool floor liner. At the upper level, the corners of four adjacent FSR are coupled in both horizontal directions with an assembly crossarm. For the external FSR, only two FSR are coupled in both the upper and lower levels.

The first part of this report develops a detailed analysis of one FSR by considering the most conservative analysis loads and boundary conditions. A detailed stress state of the different parts of the FSR is then obtained.

The second part of this report covers the evaluation of the dynamic behavior of the FSR as a freestanding structure, which is influenced by the surrounding FSR. Also analyzed are the link conditions between FSR and the hydrodynamic effects of the submergence in the pool water. The maximum displacements of the FSR and impact load reactions considering the freestanding boundary conditions are then obtained.

A design requirement of the analysis is to ensure that no interaction occurs between the FSR and pool walls (ID 4).

1.1.2 Scope

The scope of this document covers the design principles, load analysis, and justification of the configuration of the FSR assembly.

The analysis includes the results of the relative displacements between the FSR feet and the pool floor liner (sliding and uplifting), the maximum reactions between the FSR feet and the pool floor (through the lower bearing pad), and the maximum transmission forces between two FSRs at both the upper and lower links. In addition, the maximum lateral forces between fuel

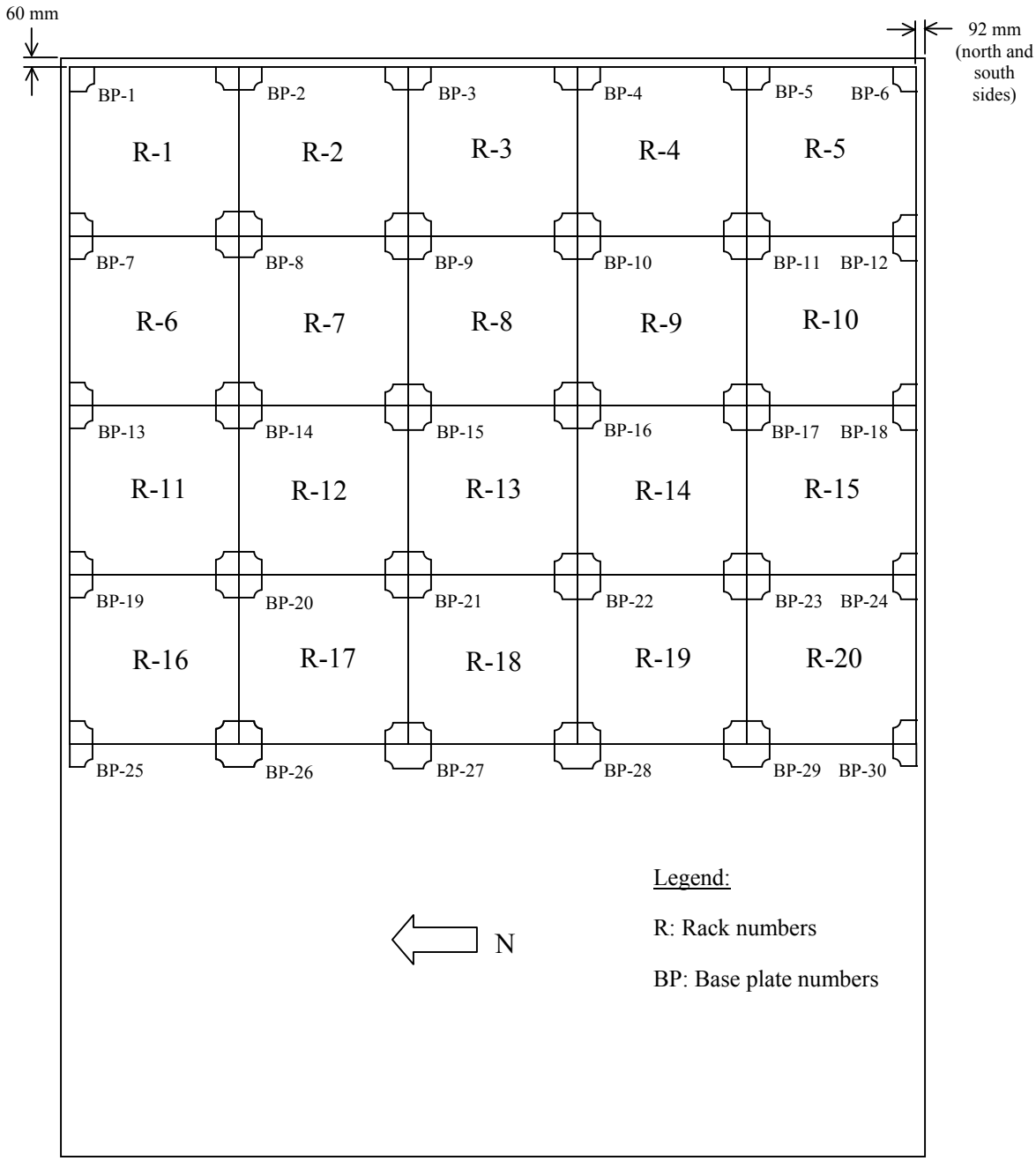

Figure 1-1. Layout of Fuel Support Racks and Base Plates

SSE	Safe Shutdown Earthquake
SRVD	Safety Relief Valve Discharge
LOCA	Loss of Coolant Accident
L_R	Lifting FSR during installation

1.4.5.1 Dead Weight + Buoyancy (D)

In addition to the dead weight of the FSR and fuel assemblies, it is also necessary to consider buoyancy, that is, the thrust that the water applies on the FSR and the immersed fuel. This effect is taken into account in the analysis by reducing the gravity acceleration by a reducing factor obtained as follows (calculation based on 15x12 size):

FSR steel mass: $M_s = 2554+1069+1885+4836 = 10344$ kg (see Table 1-6)

Steel volume: $V_s = M_s / \rho = 10344/7850 = 1.3\ m^3$

Fuel assemblies, mass: $M_f = 245*180 = 44100$ kg (ID 4)

Fuel assemblies, volume: $V_f = 0.03*180 = 5.4\ m^3$ (ID 4)

Total mass: $M_T = 10344+44100 = 54444$ kg

Total volume: $V_T = 1.3+5.4 = 6.7\ m^3$

This means a total of 6700 kg of water mass moved. Thus, the reducing factor is:

$$F = (54444-6700)/54444 = 0.876$$

And the reduced gravity acceleration is obtained from

$$g' = 0.876 \cdot g = 8.6\ m/s^2$$

1.4.5.2 Fuel Handling Loads (P_f)

The FSR will be designed to withstand a pull-up force of 17.79 kN, which is necessary in the event of a fuel assembly or grappling device hanging up during removal and a horizontal force of 4.45 kN being applied at the top of the FSR (ID 4).

1.4.5.3 Differential Temperature Induced Loads (T_o, T_a)

The maximum Spent Fuel Pool water temperatures are 48.9ºC (120ºF) in normal conditions and 60ºC (140ºF) in abnormal conditions (ID 4).

The stress-free temperature is assumed to be 15.5 ºC (ID.5).

The maximum FSR width is L=2560 mm in the N-S direction and L=2056 mm in the E-W direction (ID 1).

The maximum FSR thermal expansion, conservatively assuming a maximum temperature of 121.1°C (250ºF)(ID 4), is:

N-S direction: $\alpha \cdot L \cdot \Delta T$ = 16.4 E-6*2560*(121.1-15.5) = 4.43 mm

E-W direction: $\alpha \cdot L \cdot \Delta T$ = 16.4 E-6*2560*(121.1-15.5) = 3.6 mm

The FSRs are submerged in water and can expand in the vertical and horizontal directions without restrictions. The minimum distance between bottom FSR spacer plates is 3 mm<4.43 mm; this means one FSR could contact the FSR adjacent in the event that the water temperature will reach 121.1 ºC. Since there is enough distance to the pool walls, each FSR can expand, pushing each other. In this case the contact forces between FSRs are considerably lower than the impact forces during seismic. Therefore no thermal induced stresses are calculated in the present analysis. The temperature gradient in the vertical direction is considered negligible for structural analysis.

Maximum displacement due to the seismic event is 39.5 mm at the north and south walls and 48.9 mm at the east wall (Table 1-2). If the maximum pool temperature were to occur simultaneously with a seismic event, the resulting total displacement is calculated as:

North-south walls: 39.5 mm + 2.5(4.4) - 2(3) = 44.5 mm < 92 mm

East wall: 48.9 mm + 2(3.6) - 1.5(3) = 51.6 mm < 60 mm

As these displacements are less than the minimum horizontal distance to the pool walls, the FSRs will not impact the walls.

1.4.5.4 Safe Shutdown Earthquake (SSE)

The FSR will be designed to withstand the SSE loads. Applicable response spectra are specified in ID 4 Appendix A30. A structural damping value of 4% for SSE conditions is used (Reference 16).

For the linear analysis of the detailed model, the SSE response spectra are input directly. Figures A-1a, A-1b and A-2 show the spectra applied in the three directions.

For the non-linear analysis of the global model, the earthquake spectra are converted into three floor acceleration time histories (one for each direction)(ID 8). The acceleration versus time in the X, Y, and Z directions for SSE is shown in Figures A-3, A-4 and A-5. The total duration of the transient is 16 sec.

1.4.5.5 Safety Relief Valve Discharge (SRVD)

The FSR will be designed to withstand the SRVD loads specified in ID 4 Appendix A30. A structural damping value of 4% for SRVD conditions is used (Reference 16).

For the linear analysis of the detail model, the SRVD response spectra are input directly. Of the two applicable response spectra in the horizontal directions, X (N-S) and Y (E-W), the enveloping one (the X-direction) is chosen and conservatively applied in both horizontal

directions. Figures A-6 and A-7 in show the spectra applied in both horizontal and vertical directions.

For the reasons explained in section 1.6.1, acceleration time histories for SRVD are not obtained.

1.4.5.6 Loss of Coolant Accident (LOCA)

The FSR will be designed to withstand the LOCA loads specified in ID 4 Appendix A30. A structural damping value of 4% for LOCA conditions is used (Reference 16).

For the linear analysis of the detail model, the LOCA response spectra are input directly. Of the two applicable response spectra in the horizontal directions, X (N-S) and Y (E-W), the enveloping one (the X-direction) is chosen and conservatively applied in both horizontal directions. Figures A-8 and A-9 in show the spectra applied in both horizontal and vertical directions.

For the reasons explained in Section 1.6.1, acceleration time histories for LOCA are not obtained.

1.4.5.7 Lifting FSR During Installation (L_R)

The FSR is verified to withstand the lifting load during installation. The FSR is supported in the four base plates holes indicated in ID 1 and ID 2.

1.4.6 Load Combinations

The load combinations shall be per Appendix D of SRP 3.8.4 (Reference 8), according to ID 4. Table 1-5 shows the envelope load combinations that will be used for the design of the FSR, based on the aforementioned load combinations. Conservatively, SRVD and LOCA have also been computed in the linear analysis of the detailed model.

Table 1-5

Load Combinations

Level A:	$D + P_f$
Level D:	$D + SSE + SRVD + LOCA + T_a$ (response spectrum analysis, see Section 1.5.3)
Level D:	$D + SSE + T_a$ (transient dynamic analysis, see Section 1.6.5)

$D + P_f$ is a Level B load combination, but it is conservatively assumed as a Level A load combination.

1.4.7 Stress Limits

The stress limits are taken from ASME B&PV Code, Section III, Division I, Subsection NF (Reference 3) and Appendix F (Reference 4) corresponding to the Design by Analysis for Class 3 Plate and Shell Type Supports.

Definitions of terms are provided below as per References 3 and 4:

P_m – membrane stress (MPa)

P_b – bending stress (MPa)

τ – shear stress (MPa)

S – allowable stress (MPa)

S_u – tensile strength (MPa)

S_y – yield strength (MPa)

Base metal Type 304L (with mechanical characteristics of Type 304)

Level A Conditions (NF-3251.1 and Table NF-3552(b)-1)

$P_m \leq S = 134.1$ MPa
$P_m + P_b \leq 1.5 \cdot S = 201.1$MPa
$\tau \leq 0.6 \cdot S = 80.4$ MPa

2.4.6.4 Safe Shutdown Earthquake (SSE)

The FSR shall be designed to withstand the SSE loads specified in ID 4 Appendix A30. A structural damping value of 4% for SSE conditions is used (Reference 12). Figures A-9 and A-10 in Appendix A show the spectra applied in both horizontal and vertical directions.

2.4.6.5 Safety Relief Valve Discharge (SRVD)

The FSR shall be designed to withstand the SRVD loads specified in ID 4 Appendix A30. A structural damping value of 4% for SRVD conditions is used (Reference 12). Figures A-11 and A-12 in Appendix A show the spectra applied in both horizontal and vertical directions.

2.4.6.6 Loss of Coolant Accident (LOCA)

The FSR shall be designed to withstand the LOCA loads specified in ID 4 Appendix A30. A structural damping value of 4% for LOCA conditions is used (Reference 12). Figures A-13 and A14 in Appendix A show the spectra applied in both horizontal and vertical directions.

2.4.6.7 Lifting FSR During Installation (L_R)

The FSR is verified to withstand the lifting load during installation. The FSR is supported in the four base plate holes indicated in ID 1 and ID 2.

2.4.7 Load Combinations

The load combinations and acceptance criteria shall be per Appendix D of SRP 3.8.4. Table 2-5 shows the envelope load combinations that will be conservatively used for the design of the FSR, based on the aforementioned load combinations.

Table 2-5

Load Combinations

Level A:	$D + P_f$
Level D:	$D + SSE + SRVD + LOCA + T_a$

$D + P_f$ is a Level B load combination, but it is conservatively assumed as a Level A load combination. ~~Differential temperatures are not included in Table 2-5 due to the reasons explained in Section 2.4.6.3.~~

2.4.8 Analysis Methodology Description

Static and dynamic loads are considered in the analysis. The response spectrum analysis method is used to analyze the dynamic loads.

2.5.1 Displacement Results

The maximum horizontal displacement obtained at the top of the FSR for the most unfavorable load combinations are 2.8 mm for the X-direction, and 3.8 mm for the Y-direction (see Figures C24 and C25, respectively, in Appendix C).

One half of the expansion due to thermal expansion (Section 2.4.6.3) is applied to each rack in opposing horizontal directions. If the abnormal pool temperature were to occur simultaneously with a seismic event, the resulting total displacement is calculated as:

3.8 mm + 3.7 mm/2 = 5.7 mm

The minimum distance between adjacent FSR at the top level or between FSR and pool wall is 100 mm (ID 6). Therefore, no contact occurs between the FSR or between the FSR and the pool walls.

2.5.2 Plate Stress Results

The stress results obtained for the different load combinations are checked in the most critical sections of the different plates of the FSR. Figures C26 to C31 in Appendix C show the results.

2.5.2.1 10 mm Thick Enveloping Plate

The maximum stresses obtained on the 10mm thickness enveloping plate compared with the corresponding allowable stresses are given in Table 2-8, where:

- $S_Z \equiv$ Vertical direction (Z) membrane stress
- $S_H \equiv$ Horizontal direction (X or Y) membrane stress
- $S_{HZ} \equiv$ Shear membrane stresses on the plane of the plate.
- Bending stresses across the plate thickness are negligible and are classified as secondary stresses; however, other directions of the plate contain primary bending stresses that are included in the stress analysis results. ~~Bending plate stresses are negligible~~

Table 2-8

10mm Thickness Enveloping Plate Stress Results

Stress Category	Calculated Stress (MPa)	Allowable Stress (MPa)
Level A Conditions Maximum Membrane Stresses	$S_Z = 7.0$	134.1
	$S_H = 2.1 \times 2 = 4.2$	134.1
	$S_{HZ} = 2.2$	80.4
Level D Conditions Maximum Membrane Stresses	$S_Z = 131$ (Figure C26)	292.8
	$S_H = 35 \times 2 = 70$	292.8

3.4.6.5 Safety Relief Valve Discharge (SRVD)

The FSR shall be designed to withstand the SRVD loads specified in ID 4 Appendix A30. A structural damping value of 4% for SRVD conditions is used (Reference 12). Figures E-9 and E10 in Appendix E show the spectra applied in both horizontal and vertical directions.

3.4.6.6 Loss of Coolant Accident (LOCA)

The FSR shall be designed to withstand the LOCA loads specified in ID 4 Appendix A30. A structural damping value of 4% for LOCA conditions is used (Reference 12). Figures E-11 and E12 in Appendix E show the spectra applied in both horizontal and vertical directions in.

3.4.6.7 Lifting FSR During Installation (L_R)

The FSR is verified to withstand the lifting load during installation. The FSR is supported in the four upper holes of the tow grid upper plates (ID 1 and ID 2, item 53.001).

3.4.7 Load Combinations

The load combinations and acceptance criteria shall be per Appendix D of SRP 3.8.4. Table 3-5 shows the envelope load combinations that will be conservatively used for the design of the FSR, based on the aforementioned load combinations.

Table 3-5

Load Combinations

Level A:	$D + P_f$
Level D:	$D + SSE + SRVD + LOCA + T_a$

$D + P_f$ is a Level B load combination, but it is conservatively assumed as a Level A load combination. ~~Differential temperatures are not included in Table 3-5 due to the reasons explained in Section 3.4.6.3.~~

3.4.8 Analysis Methodology Description

Static and dynamic loads are considered in the analysis. The response spectrum analysis method is used to analyze the dynamic loads.

The static load case (D) is resolved by structural static analysis applying the reduced gravity acceleration g' (see Section 3.4.6.1).

The fuel handling load case (P_f) is analyzed by applying the forces prescribed in Section 3.4.6.2 in a central channel (see Figure E-13).

Table 3-7b indicates the acceleration considered to account for the high-frequency modes, with the corresponding percentage of missing mass.

Table 3-7b

Acceleration for Missing Masses

Event	X direction		Y direction		Z direction	
	Acceleration (g)	(%)	Acceleration (g)	(%)	Acceleration (g)	(%)
SSE	1.27	27.7	1.25	25.2	1.74	100
LOCA	0.05	31.2	0.029	19.3	0.225	100
SRVD	0.067	31.2	0.067	25.2	0.143	100

3.5.1 Displacements Results

The maximum horizontal displacement obtained at the top of the FSR for the most unfavorable load combination is 18.0 mm and occurs in the X-direction (see Figure A-24, in Appendix A).

One half of the expansion due to thermal expansion (Section 3.4.6.3) is applied to each rack in opposing horizontal directions. If the abnormal pool temperature were to occur simultaneously with a seismic event, the resulting total displacement is calculated as:

18.0 mm + 5.9 mm/2 = 21.0 mm

The minimum distance between adjacent FSR at the top level or between FSR and pool wall is 100 mm (ID 6). Therefore, no contact occurs between adjacent FSR or between the FSR and the pool walls.

3.5.2 Plate Stress results

The stress results obtained for the different load combinations are checked in the most critical sections of the different plates of the FSR. Figures E-25 to E-28 in Appendix E show the results.

3.5.2.1 8 mm Thick Channel Plate

The maximum stresses obtained for the 8mm thick channel plate compared with the corresponding allowable stresses are given in Table 3-8, where:

- $S_Z \equiv$ Vertical direction (Z) membrane stress
- $S_H \equiv$ Horizontal direction (X or Y) membrane stress
- $S_{HZ} \equiv$ Shear membrane stresses on the plane of the plate.

A 42 mm gap between the racks and the northern and southern pool walls has been included in the model. No gap has been considered between the racks and the eastern pool wall. Nor was any gap considered between racks. The gaps used in the model are conservative relative to actual design values.

5.2.3.1 Loss Coefficient Calculation

Figure 5-2 (Reference 8) shows the loss coefficient in the vertical direction inside the racks. This curve is mathematically fit using the following parabolic expression:

$$y = ax^2 + bx + c$$

Where:

y is the pressure drop (PSI)

x is the mass flow rate (LBM/hr)

Since there is no pressure drop when the mass flow rate is zero, $c = 0$. From the parabolic fitting, the coefficients values are:

$$b = 0$$

$$a = 6.2 \cdot 10^{-10}\ PSI\ \frac{hr^2}{LBM^2} = 269.55\ \frac{1}{kg \cdot m}$$

Thus, pressure loss can be represented by the following formula:

$$\Delta P = K \cdot (\dot{m})^2$$

Where:

$$K = 269.55 Kg^{-1} \cdot m^{-1}$$